Trapping against hydrogen embrittlement

Conference Paper · August 2017

CITATIONS
6

READS
831

6 authors, including:

Zahra S. Hosseini
University of Illinois Urbana-Champaign
9 PUBLICATIONS **97** CITATIONS
SEE PROFILE

Petros Sofronis
University of Illinois Urbana-Champaign
144 PUBLICATIONS **11,881** CITATIONS
SEE PROFILE

TRAPPING AGAINST HYDROGEN EMBRITTLEMENT

ZAHRA S. HOSSEINI[1]
University of Illinois at Urbana-Champaign, Urbana, IL, USA

MOHSEN DADFARNIA[1]
University of Illinois at Urbana-Champaign, Urbana, IL, USA

KEVIN A. NIBUR
Hy-Performance Materials Testing, Bend, OR, USA

BRIAN P. SOMERDAY[1]
Southwest Research Institute, San Antonio, TX, USA

RICHARD P. GANGLOFF
University of Virginia, Charlottesville, VA, USA

PETROS SOFRONIS[1]
University of Illinois at Urbana-Champaign, Urbana, IL, USA

[1] International Institute for Carbon-Neutral Energy Research (I^2CNER)

ABSTRACT

Petrochemical pressure vessels operating in high pressure H_2 at high temperature suffer from hydrogen embrittlement (HE) during repressurization after shutdown cooling to ambient temperature. HE may be mitigated by introduction of hydrogen (H) traps in the steel microstructure to suppress accumulation of H necessary for embrittlement at fracture initiation sites. Experimentally, nano-scale vanadium carbides (VC) significantly improve the HE resistance of bainitic steel specific to closed system H introduced by elevated temperature exposure to H_2. To understand the effect of VC precipitates on HE of 2¼Cr-1Mo-¼V steel, we analyze re-partitioning of H among various trap states, first as a function of temperature during cooling from high temperature, then during loading of a cracked body in moist air. Results show that VC precipitates deplete lattice-H concentration during cooling, and markedly reduce the H population in lath boundaries that are process zone fracture sites. Either reduction in H concentration is consistent with improved HE resistance.

INTRODUCTION

Hydrogen embrittlement (HE) is a severe environment-sensitive failure mode [1,2,3] observed in petrochemical industries. Thick wall alloy steel pressure vessels exposed to high pressure hydrogen gas (10–20 MPa) at elevated temperature (300–480°C) are susceptible to hydrogen (H) uptake that can lead to HE after shut-down to room temperature and near-0 H_2 pressure followed by H_2 repressurization [4]. An approach to mitigate such "closed-system" HE is based on introduction of hydrogen (H) traps in the steel microstructure to attract diffusible H, thus making it unavailable to partition to locations where it initiates fracture [5,6]. Carbide-forming elements (Ti, Mo, V, W, or Nb) promote finely-dispersed nano-scale precipitates that may improve the HE resistance of steel [7,8]. Vanadium carbides (VC), sized on the order of 20 nm, readily precipitate in thick-section bainitic Cr-Mo steel plate and weld metal, and act as strong-reversible H-trap sites [9]. Mitigation of HE in refinery pressure vessels is, in

part, based on replacement of 2¼Cr-1Mo steel by 2¼Cr-1Mo-¼V. Figure 1 shows that the fracture resistance of modern temper embrittlement resistant 2¼Cr-1Mo steel base plate and weld metal (yield strength = 510 to 550 MPa) decreases dramatically with increasing hydrogen concentration [10]. However, V-modified Cr-Mo steel of similar strength resists HE to at least K_{IH} of 140 MPa√m, even for a total-dissolved hydrogen concentration above 9 wppm [11].

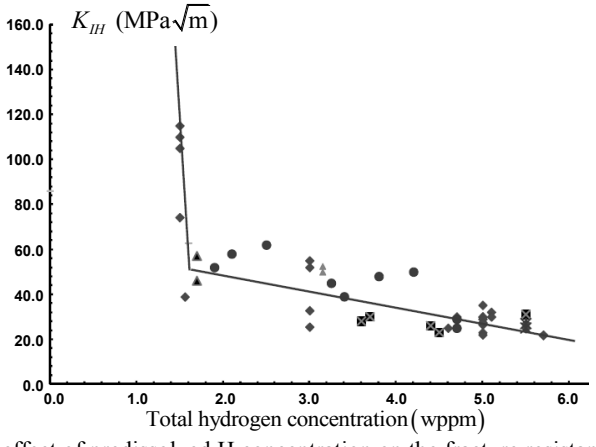

Figure 1. The effect of predissolved H concentration on the fracture resistance, K_{IH}, of H_2 precharged compact tension specimens of modern (high purity) 2¼Cr-1Mo steel stressed in moist air at 23-25ºC. K_{IH} is the stress intensity at the onset of subcritical crack growth under slow-rising displacement at dK/dt of 0.007 MPa√m/s. Different symbols represent experimental data from different laboratories [10].

In this work, we elucidate the role of VC precipitates in the HE resistance of V-modified steel. The first step is to understand H re-partitioning among various traps during cooling from a high charging temperature to ambient temperature in the absence of external loading. To accomplish this, we modify the H transport equation under constant temperature [12] to account for the temperature effect on the re-partitioning of H among lattice and multiple trapping sites with varying H-trap binding energy. Next, we calculate the effect of VC precipitates on the development of H populations upon loading at 25ºC. The idea is to understand how applied load interacts with H distributed in the crack tip fracture process zone, in the absence or presence of potentially beneficial trap states, and to ascertain the relationship of these H populations to HE of these steels.

HYDROGEN TRANSPORT IN AN ELASTOPLASTICALLY DEFORMING MATERIAL UNDER VARYING TEMPERATURE

Hydrogen atoms reside in either normal interstitial lattice sites (NILS) or trap sites. The occupancy of the jth type of trap, $\theta_T^{(j)}$, is assumed in equilibrium with NILS occupancy, θ_L, according to Oriani's theory [13] such that

$$\frac{\theta_T^{(j)}}{1-\theta_T^{(j)}} = \frac{\theta_L}{1-\theta_L} K_T^{(j)}, \quad K_T^{(j)} = \exp\left(\frac{W_B^{(j)}}{RT}\right), \tag{1}$$

where $K_T^{(j)}$ is the equilibrium constant calculated from the corresponding H-trap binding energy $W_B^{(j)}$, R (8.314 J/mol K) is the gas constant, and T is absolute temperature. The hydrogen concentration in trap type (j) is expressed as $C_T^{(j)} = \alpha^{(j)}\,\theta_T^{(j)}\,N_T^{(j)}$, where $\alpha^{(j)}$ is the number of sites per trap type (j), and $N_T^{(j)}$ is the corresponding trap density per unit volume. The hydrogen concentration in NILS, measured in hydrogen atoms per unit volume, is $C_L = \beta\,\theta_L\,N_L$, where β is the number of NILS per solvent atom, $N_L = N_A / V_M$ represents the density of solvent atoms, N_A is Avogadro's number, and V_M is the molar volume of the host lattice.

Following Sofronis and McMeeking [14], we obtain the hydrogen transport equation for stress-driven diffusion accounting for the temperature effect on the equilibrium between trapping site and NILS concentrations

$$\frac{D}{D_{eff}}\frac{\partial C_L}{\partial t}+\sum_j\left(\alpha^{(j)}\theta_T^{(j)}\frac{dN_T^{(j)}}{d\varepsilon^p}\right)\frac{d\varepsilon^p}{dt}-\sum_j\left(\frac{C_L\alpha^{(j)}N_T^{(j)}W_B^{(j)}K_T^{(j)}(\beta N_L-C_L)}{[\beta N_L+(K_T^{(j)}-1)C_L]^2RT^2}\right)\frac{\partial T}{\partial t}$$
$$-DC_{L,ii}+\left(\frac{DV_H}{3RT}C_L\sigma_{kk,i}\right)_{,i}=0\,, \qquad (2)$$

where $(\,)_{,i}=\partial(\,)/\partial x_i$, $\partial/\partial t$ is partial differentiation with respect to time, a repeated index implies the standard summation convention over the range, D is the H diffusion coefficient through NILS, D_{eff} is an effective diffusion coefficient [12], ε^p and σ_{ij} are the effective plastic strain and the Cauchy stress respectively, and V_H is the partial molar volume of hydrogen in solution. Equation (2) shows that the distribution of H within the crack tip plastic and process zones depends on elastoplastic deformation. The steel is considered to harden isotropically and obey von Mises yielding with an associated flow rule. For the coupling of the material deformation about the crack tip with the H transport, the approach presented by Sofronis and McMeeking [14] is followed.

HYDROGEN RE-DISTRIBUTION UPON COOLING TO ROOM TEMPERATURE AND SUBSEQUENT LOADING

We simulated H re-partitioning among traps and lattice sites in 2¼Cr-1Mo and 2¼Cr-1Mo-¼V steels during cooling (closed system without stress) from the charging temperature to 25ºC. Samples were assumed to be thermally charged at an H_2 pressure (P) of 18 MPa and temperature T of 723 K to produce an equilibrium concentration of uniformly distributed H. Based on experimental measurements [11] of the total amount of H dissolved at this charging condition, we considered a total H concentration of 4.5 and 9.5 wppm for the baseline Cr-Mo and V-modified steels, respectively. The lattice H concentration at the charging condition (C_{Lc}) is calculated through Sieverts law for pure iron, $C_{Lc} = 0.00185\sqrt{f}\exp(-\Delta H/RT)$, to be 3.9 wppm, where the heat of solution (ΔH) is 28.6 kJ/mol [1], fugacity (f) is $P\exp(Pb/RT)$ [15], and b = 15.84 cm^3/mol for H_2. To calculate H re-partitioning upon cooling, Eq. (2) was solved using a domain with this initial H distribution, and zero stress and deformation fields. Since the thickness of the pressure vessel is large, 10-35 cm, we assumed that H does not escape from the simulation domain upon cooling, which is associated with a

zero flux boundary condition on the external boundary.

Based on the bainitic microstructure of 2¼Cr-1Mo steel [5,6], we considered four H-trap states: prior austenite grain boundaries, lath interfaces, dislocations, and relatively large carbides, $(Cr,Fe)_7C_3$. 2¼Cr-1Mo also contains large $(Cr,Fe)_6C$ and $(Cr,Fe)_2C$ carbides, but the dominant carbide is $(Cr,Fe)_7C_3$. Thermal desorption spectroscopy (TDS) measurements of the binding energy for $(Cr,Fe)_7C_3$ traps in 2¼Cr-1Mo steel are lacking. However, convincing data for similar carbides in a Ni superalloy support a H-trap binding energy of 50 kJ/mol [16]. With this trap binding energy, $W_B^{(C)}$ = 50 kJ/mol, we calculated the corresponding H trap site density associated with carbides as 4.6×10^{24} sites/m from the fact that the total amount of H at the charging condition is 4.5 wppm. The material properties and characteristics of these trap states for 2¼Cr-1Mo are shown in Table 1. The H trap site densities and $W_B^{(j)}$ for carbides, grain boundaries, and lath boundaries are assumed to remain unchanged upon cooling. However, during subsequent loading, the dislocation trap density increases in the crack tip plastic and fracture process zones. Assuming one H trap site per atomic plane threaded by a dislocation line [17,18], we obtain the dislocation trap density as a function of the dislocation density, ρ, and the Fe lattice parameter, a, by $N_T^{(D)} = \sqrt{2}\,\rho/a$, where dislocation density is assumed to be proportional to plastic strain ε^p as reported in [12,19].

Table 1. Material properties of bainitic 2¼Cr-1Mo steel

Properties	Symbol	Value
Young's modulus (GPa)	E	200
Yield stress (MPa)	σ_0	550
Poisson's ratio	ν	0.3
Work hardening exponent	n	0.04
Molar volume of the host lattice (cm^3/mol)	V_M	7.116
Number of NILS per solvent atom	β	1
Partial molar volume of hydrogen (cm^3/mol)	V_H	2 [1]
Diffusion coefficient (m^2/s)	D	1.271×10^{-8} [1]
Solubility at 300 K (mol H_2 /$m^3\sqrt{MPa}$)	K	5.434×10^{-3} [1]
Grain boundary trap binding energy (kJ/mol)	$W_B^{(GB)}$	60 [1]
Lath boundary trap binding energy (kJ/mol)	$W_B^{(Lath)}$	38 [6]
Dislocation trap binding energy (kJ/mol)	$W_B^{(D)}$	20.2 [1]
Carbide trap binding energy (kJ/mol)	$W_B^{(C)}$	50 [16]
Grain boundary H trap site density (H sites/m^3)	$\alpha^{(GB)} N_T^{(GB)}$	10^{23} [1]
Lath boundary H trap site density (H sites/m^3)	$\alpha^{(Lath)} N_T^{(Lath)}$	5×10^{24} [6]
Dislocation H trap site density (no plastic deformation) (H sites/m^3)	$\alpha^{(D)} N_T^{(D)}$	4.93×10^{19} [12,19]
Carbide H trap site density (H sites/m^3)	$\alpha^{(C)} N_T^{(C)}$	4.6×10^{24}
Lattice parameter (nm)	a	0.286

For bainitic 2¼Cr-1Mo-¼V steel, material properties were assumed to be the same as for 2¼Cr-1Mo (Table 1), with the only difference being the nano-scale VC precipitate traps from aging at 600-700ºC, and associated reduction in D_{eff} from trapping theory [11,12]. VC was assumed to have a $W_B^{(VC)}$ of 35 kJ/mol [9], independent of temperature. The corresponding H trap site density ($\alpha^{(VC)}N_T^{(VC)}$) was calculated to be 3.43×10^{26} H sites/m^3 such that the total H concentration at the H_2 charging condition matches the measured value of 9.5 wppm.

ROLE OF VC PRECIPITATES IN HYDROGEN RE-DISTRIBUTION UPON COOLING

H partitions to various trap states during cooling to room temperature, as shown by model predictions of normalized H concentration in Fig. 2. The concentration of H in NILS is depleted by partitioning to nano-scale VC in V-modified Cr-Mo (e.g., C_L = 0.00167 wppm at 25ºC, Fig. 2c), but is high in the baseline steel (C_L = 2.45 wppm at 25ºC, Fig. 2a). The H concentrations at dislocations and grain boundaries at 25ºC are on the order of 10^{-7} and 10^{-2} wppm, respectively, for baseline and V-modified steels, and do not change

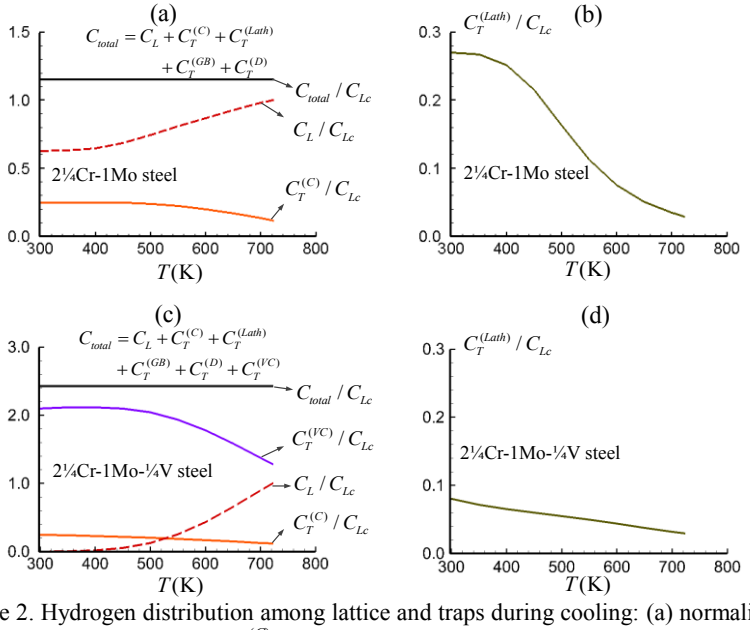

Figure 2. Hydrogen distribution among lattice and traps during cooling: (a) normalized H concentration at carbides, $C_T^{(C)}/C_{Lc}$, and in the lattice, C_L/C_{Lc} for 2¼Cr-1Mo; (b) $C_T^{(Lath)}/C_{Lc}$ at lath boundaries, for 2¼Cr-1Mo; (c) normalized H concentrations at carbides, VC, $C_T^{(VC)}/C_{Lc}$, and NILS for 2¼Cr-1Mo-¼V; (d) $C_T^{(Lath)}/C_{Lc}$ at lath boundaries for 2¼Cr-1Mo-¼V. At the charging condition (P = 18 MPa and T = 723 K), the total amount of H is C_{total} = 4.5 and 9.5 wppm respectively for 2¼Cr-1Mo and 2¼Cr-1Mo-¼V steels, and the initial NILS concentration is C_{Lc} = 3.9 wppm for both steels.

significantly during cooling. If lattice H causes crack tip process zone damage, then the HE resistance of V-modified steel should increase as C_L is depleted by strong H trapping at the VC precipitates. Alternately, the H concentration at lath boundary traps is lower for the V-modified steel, at ambient temperature and in equilibrium with the lower lattice H content [13], compared to Cr-Mo steel; see Figs. 2b and 2d. Lath boundaries constitute a H-crack path in Cr-Mo steel that is not temper embrittled [5,6]; as such, reduced H at lath boundaries in V-modified steel could result in improved HE resistance.

EFFECT OF LOADING ON RE-PARTITIONING OF HYDROGEN AMONG CRACK TIP TRAP STATES AND LATTICE SITES

Hydrogen re-partitioning in precharged and cooled 2¼Cr-1Mo and 2¼Cr-1Mo-¼V, due to loading at 25 ºC, was analyzed. To simulate the H population development in a compact tension (CT) specimen, we used finite element analysis to solve the coupled deformation and hydrogen transport problems, Eq. (2), under small scale yielding (SSY, Fig. 3). We assumed plane strain and an initial crack tip opening displacement, b_0, of 10 μm. The outer boundary of the SSY domain, located at a distance of L = 50 mm from the crack tip, was loaded by Irwin's Mode I asymptotic displacements [20]. These displacements were applied incrementally to achieve a constant stress intensity rate, dK_I/dt, of 10^{-4} MPa√m/s from the stress-free state to the final K_I of 40 MPa√m, which approximates the failure load for the baseline steel in Fig. 1. The calculated H distribution upon cooling to ambient temperature served as the initial conditions for the lattice and trap site H populations. The external surface and crack faces were assumed impermeable to hydrogen loss, and H uptake during loading in either moist air or low pressure residual H_2 was not modeled.

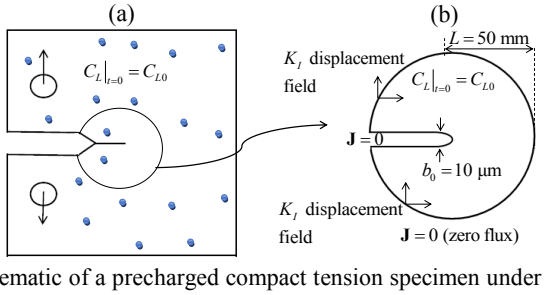

Figure 3. (a) Schematic of a precharged compact tension specimen under load and (b) the domain of analysis, and the boundary and initial conditions, for the SSY simulation of H re-partitioning upon loading. The parameter, C_{L0}, is the NILS H concentration at the start of loading at room temperature.

Figure 4 shows the H concentration profiles at NILS and lath boundaries, along the axis of symmetry ahead of the crack tip at the end of loading (K_I = 40 MPa√m) for the baseline and V-modified steels. The H concentration in lattice sites in the 2¼Cr-1Mo-¼V specimen is about 3 orders of magnitude less than that in the 2¼Cr-1Mo CT specimen. In addition, H trapped at lath boundaries in the V-modified specimen exhibits a factor of 3 decrease in comparison to that in

the baseline steel. These results indicate that VC precipitates are a critical feature of the steel microstructure, depleting the H concentration partitioned to lattice and all other trap states. In particular, note that VC precipitates markedly reduce the H population in lath boundaries, which as discussed, serve as fracture initiation sites. Hence, VC precipitates are suggested to improve HE resistance; the basis for this improvement is that uniformly distributed nano-scale VC precipitates act as strong traps, which attract H. A consequence of this analysis is the implication that addition of VC precipitates effectively shifts HE susceptibility to higher-initial levels of C_{Lc}, as produced by either higher hydrogen pressure or higher temperature during pressure vessel operation. Moreover, these results provide a basis for simulating the effect of loading temperature on HE due to precharged hydrogen [10].

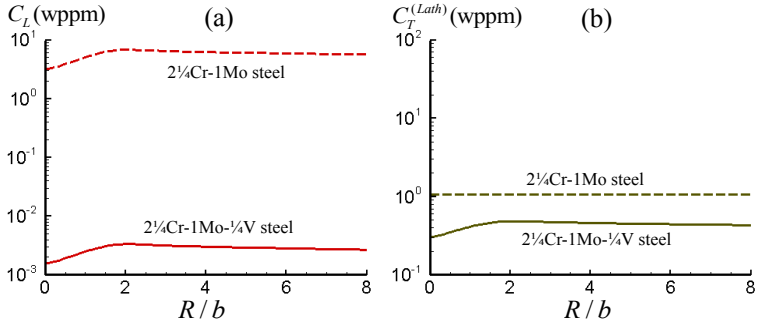

Figure 4. Plot of H concentration vs. normalized distance, R/b, from the crack tip at K_I = 40 MPa√m for 2¼Cr-1Mo and 2¼Cr-1Mo-¼V steels. (a) Lattice H concentration, C_L, and (b) H concentration at lath boundaries, $C_T^{(Lath)}$. The calculated crack opening displacement at the end of loading is b = 39.6 μm.

DISCUSSION

Two issues must be examined by future research, uncertain $W_B^{(VC)}$ (and $\alpha^{(VC)} N_T^{(VC)}$) and open system behavior. First, the predicted H concentrations in Figs. 2 and 4 are sensitive to $W_B^{(VC)}$, which depends on Cr-Mo-V aging temperature and charging temperature [21], but these dependencies are not known. The VC trap energy used for modeling, 35 kJ/mol, is the measured activation energy for H desorption during TDS of martensitic Fe-1.5Mn-0.25C-0.30 V (wt pct) aged at 600ºC and H precharged at 25ºC [9]. However, desorption energy must be reduced by the energy of H migration in the lattice, about 10 kJ/mol [22], to yield an accurate $W_B^{(VC)}$ of 25 kJ/mol. H permeation measurements at 25ºC with ferritic Fe-0.08C-0.19V (aged at 600ºC) yielded $W_B^{(VC)}$ of 17.5 kJ/mol [23], and TDS showed that $W_B^{(i)}$ is as low as 12 kJ/mol for coherent $(Cr,Mo)_2C$ precipitates in steel precharged at 25ºC [22]. These lower $W_B^{(C)}$ values are not relevant to high temperature charging of Cr-Mo-V. In fact, sensitivity calculations with $W_B^{(VC)}$ less than 35 kJ/mol gave unrealistically high VC trap density.

Unique-strong H trapping occurs at VC precipitates when H is introduced at elevated temperatures, compared to significant but lower $W_B^{(VC)}$ trapping in Cr-Mo-V electrochemically precharged at 25ºC [24]. Elevated temperature appears to provide sufficient activation energy for H to enter the bulk-VC lattice, with possible trapping at interface sites, as suggested by Pillot et al. [24] and detailed by Wei and Tsuzaki for TiC [21]. (The $W_B^{(TiC)}$ for H trapped in the TiC lattice is 53 kJ/mol with a trap density of 7.1×10^{25} sites/m^3 per 1 vol pct of TiC [21].) With such high $W_B^{(VC)}$, H detrapping from intra-VC lattice sites is impeded at temperatures below about 100ºC, consistent with measured-slow H outgassing (and very low D_{eff}) for Cr-Mo-V [24]. In contrast, charging at 25ºC produces H trapping at VC interfaces, characterized by a lower $W_B^{(VC)}$ (perhaps in the range of 18-25 kJ/mol) and higher D_{eff} at 25ºC. These considerations justify use of the high H-trap binding energy of 35 kJ/mol for H repartitioning during cooling and subsequent loading at ambient temperature. None-the-less, TDS measurements are required for Cr-Mo-V, H_2 precharged at elevated temperature (400-500ºC), as well as aged at higher temperatures (~700ºC), relevant to petrochemical applications. (Interface coherence and carbide-lattice vacancy concentration depend on aging temperature and impact H trapping [21].) Alternately, VC trap density must be determined by electron microscopy or phase equilibrium modeling so $W_B^{(VC)}$ can be calculated by matching measured C_{Lc} from elevated temperature H_2 charging. Finally, D_{eff} measured versus temperature [11,24] provides an approach to calibrate $W_B^{(VC)}$ or VC trap density using Eq. (2).

Second, the present simulation of the benefit of VC trapping is relevant to HE under closed system boundary conditions [1]. In contrast, for an open system, one trap state does not affect the concentrations of H partitioned to other traps. Under open system charging, VC precipitates should not reduce lattice or lath interface trap site H concentrations for Cr-Mo-V compared to Cr-Mo, as confirmed by calculations using the material properties discussed previously (see Table 1).[1] It follows that VC precipitates will not affect K_{IH} for slow-loading in H_2 or aqueous H-producing environments, or for 25ºC charging followed by loading in air, since all crack tip trap states fill according to each $W_B^{(j)}$. This projected behavior is supported by experiments [24]; K_{IH} from J-integral resistance curve measurements is very high for Cr-Mo-V precharged in elevated temperature H_2 to a total H concentration of 7.5-9.5 wppm, consistent with the results that motivated the present modeling [11]. In contrast, K_{IH} is among the lowest values measured for Cr-Mo-V precharged in acidic-H_2S solution at 25ºC (total H concentration of 4.3 wppm). Equally high HE susceptibility is reported for 2¼Cr-1Mo steel (see Fig. 1), independent of

[1] Calculations simulated open system exposure of Cr-Mo and Cr-Mo-V in high P (69 MPa) to approximate the H fugacity associated with charging in the acidic-H_2S solution at 25ºC. The resulting H concentrations are: (a) C_L of 0.0105 wppm for Cr-Mo and Cr-Mo-V, (b) $C_T^{(Lath)}$ of 0.77 wppm for Cr-Mo and Cr-Mo-V, and (c) $C_T^{(VC)}$ of 32.3 wppm for Cr-Mo-V. Predicted total H concentrations of 1.8 wppm and 34.1 wppm are well aligned with measurements of 1.9 wppm and 4.3 wppm [24] for Cr-Mo and Cr-Mo-V, respectively. The predicted-high $C_T^{(VC)}$ is due to the high $W_B^{(VC)}$ used in the simulation; as discussed, the binding energy for ambient temperature H trapping is likely in the range of 18-25 kJ/mol rather than 35 kJ/mol.

charging temperature. This poor HE resistance of Cr-Mo-V steel, precharged at ambient temperature, is attributed to equilibrium filling of lattice and lath interface trap sites, with no benefit of VC trapping. These trap site H concentrations exceed the shielded levels associated with elevated temperature precharged and cooled steel (see Footnote 1 compared to Figs. 2 and 4). The strong-benefit of VC trapping of H, shielding Fe lattice and lath interface trap states from H localization during cooling from elevated temperature charging, is eliminated when VC precipitates are either not present (2¼Cr-1Mo steel) or when aged 2¼Cr-1Mo-¼V is precharged at ambient temperature to preclude high $W_B^{(VC)}$ H trapping.

CONCLUSIONS

We present a mechanistic explanation for the better HE resistance of elevated temperature H precharged 2¼Cr-1Mo-¼V steel compared to 2¼Cr-1Mo. A closed system analysis is based on a model of H transport in an elastoplastically deforming solid that accounts for varying temperature, stress, and plastic strain. We explore H re-partitioning among various trap states and lattice sites during cooling from a high charging temperature to ambient in both steels. The results show that VC precipitates deplete lattice sites of H and reduce the H concentration trapped at lath boundaries that are fracture initiation sites. The loading effect on H redistribution, ahead of a crack tip and after cooling, is explored by solving the coupled H diffusion and elastoplastic boundary value problems for the compact tension specimen. Results show that homogeneously distributed VC precipitates increase the resistance of 2¼Cr-1Mo-¼V to closed-system HE by strongly gathering H from lattice sites and lath interface trap states, consistent with published experiments. This mechanism to mitigate HE is specific to elevated temperature H precharging that promotes a high H-trap binding energy, and does not impact H cracking under open-system conditions such as produced by ambient temperature precharging, or by H_2 at the crack tip during loading.

ACKNOWLEDGEMENTS

ZSH, MD, BPS, and PS acknowledge the support of the International Institute for Carbon-Neutral Energy Research (WPI-I^{2}CNER), sponsored by the World Premier International Research Center Initiative (WPI), MEXT, Japan.

REFERENCES

[1] Hirth, J. P., 1980, "Effects of hydrogen on the properties of iron and steel," *Metallurgical Transactions A*, 11(6), pp. 861-890.

[2] Birnbaum, H. K., Robertson, I. M., Sofronis, P., and Teter, D., 1997, "Mechanisms of hydrogen related fracture—a review," *Second International Conference on Corrosion Deformation Interactions,* T. Magnin, ed., Institute of Materials, Great Britain, pp. 172–195.

[3] Gangloff, R. P., and Somerday, B. P., eds., 2012, *Gaseous Hydrogen Embrittlement of Materials in Energy Technologies*, Vol. 1 and Vol. 2, Woodhead Publishing Ltd, Oxford, UK.

[4] Pillot, S., and Coudreuse, L., 2012, "Hydrogen-induced disbonding and embrittlement of steels used in petrochemical refining," *Gaseous Hydrogen Embrittlement of Materials in Energy Technologies*, Vol. 1, R. P. Gangloff and B. P. Somerday, eds., Woodhead Publishing Ltd, Oxford, UK, pp. 51-93.
[5] Gangloff, R. P., 2000, "Laboratory studies of hydrogen embrittlement in aging Cr-Mo steel for thick-wall reactors," *Final Report, Phase I JIP on Aging Hydroprocessing Reactors*, Chevron Materials Engineering, Richmond, VA.
[6] Al-Rumaih, A. M., 2004, "Measurement and modeling of temperature dependent hydrogen embrittlement of Cr-Mo steel to enable fitness-for-service modeling," PhD Dissertation, University of Virginia, Charlottesville, VA.
[7] Pressouyre, G. M., and Bernstein, I. M., 1978, "A quantitative analysis of hydrogen trapping," *Metallurgical Transactions* A, 9(11), pp. 1571-1580.
[8] Takahashi, J., Kawakami, K., Kobayashi, Y., and Tarui, T., 2010, "The first direct observation of hydrogen trapping sites in TiC precipitation-hardening steel through atom probe tomography," *Scripta Materialia*, 63(3), pp. 261-264.
[9] Asahi, H., Hirakami, D., and Yamasaki, S., 2003, "Hydrogen trapping behavior in vanadium added steel," *ISIJ International*, 43(4), pp. 527-533.
[10] Al-Rumaih, A. M., and Gangloff, R. P., 2014, "Measurement and modeling of temperature dependent internal hydrogen assisted cracking in Cr-Mo Steel," *Hydrogen-Materials Interactions*, B. P. Somerday and P. Sofronis, eds., ASME Press, New York, NY, pp. 33-48.
[11] Pillot, S., Nibur, K. A., and Gangloff, R. P., 2014, "Hydrogen Cracking of Cr-Mo-V Steel from High Pressure H_2 Service," *Proceedings of 2nd International Conference on Metals and Hydrogen*, L. Duprez and Z. Zermout, eds., OCAS, Ghent, Belgium, pp. 433-447.
[12] Dadfarnia, M., Sofronis, P., and Neeraj, T., 2011, "Hydrogen interaction with multiple traps: Can it be used to mitigate embrittlement?" *International Journal of Hydrogen Energy*, 36(16), pp. 10141-10148.
[13] Oriani, R. A., 1970, "The diffusion and trapping of hydrogen in steel," *Acta Metallurgica*, 18(1), pp. 147-157.
[14] Sofronis, P., and McMeeking, R. M., 1989, "Numerical analysis of hydrogen transport near a blunting crack tip," *Journal of the Mechanics and Physics of Solids*, 37(3), pp. 317–350.
[15] San Marchi, C., Somerday, B. P., and Robinson, S. L., 2007, "Permeability, solubility and diffusivity of hydrogen isotopes in stainless steels at high gas pressures," *International Journal of Hydrogen Energy*, 32(1), pp. 100–116.
[16] Young, G. A., and Scully, J. R., 1997, "Evidence that carbide precipitation produces hydrogen traps in Ni-17Cr-8Fe alloys," *Scripta Materialia,* 36(6), pp. 713-719.
[17] Tien, J. K., Thompson, A. W., Bernstein, I. M., and Richards, R. J., 1976, "Hydrogen transport by dislocations," *Metallurgical Transactions A*, 7(6), pp. 821-829.
[18] McLellan, R. B., 1979, "Thermodynamics of diffusion behavior of interstitial solute atoms in non-perfect solvent crystals," *Acta Metallurgica*, 27(10), pp. 1655-1663.
[19] Gilman, J. J., 1969, *Micromechanics of Flow in Solids*, McGraw-Hill, New York, NY.
[20] Irwin, G. R., 1960, "Fracture mechanics," *Proceedings of 1st Symposium of Naval Structural Mechanics*, J. N. Goodier and N. J. Hoff, eds., Pergamon Press, New York, NY, pp. 557-594.
[21] Wei, F.G. and Tsuzaki, K., 2012, "Hydrogen trapping phenomena in martensitic steels," *Gaseous Hydrogen Embrittlement of Materials in Energy Technologies*, Vol. 1, R. P. Gangloff and B. P. Somerday, eds., Woodhead Publishing Ltd, Oxford, UK, pp. 493-525.
[22] Li, D., Gangloff, R. P., and Scully, J. R., 2004, "Hydrogen trap states in ultrahigh-strength AerMet 100 steel," *Metallurgical and Materials Transactions*, 35(3), pp. 849-864.
[23] Grabke, H. J., and Riecke, E., 2000, "Absorption and diffusion of hydrogen in steels," *Materials Technology*, 34 (6), pp. 331-342.
[24] Pillot, S., Corre, S., Heritier, D., Coudreuse, L., and Toussaint, P., 2014, "Effect of hydrogen charging method on fracture properties of 2¼Cr-1Mo(-V) alloys—Application of fracture mechanics concepts—Review of available data", Paper No. 04029, *Corrosion 2014*, NACE International, Houston, TX.